論文・報告

ロータブレードのねじり荷重の同定

Rotor Blade Torsional Load Identification

ジェリー　ヒグマン
Dr. Jerry P. HIGMAN
川田工業㈱航空事業部開発室技術開発課

ヘリコプタのロータブレード上のねじり荷重分布を同定法により計算する方法を開発，検証した。この方法はブレードの動的応答の実測値を併用して，ブレードの荷重状態，ねじり角および空力モーメントを計算する。方程式の解法は逆転送行列法に基づいている。またブレードの運動方程式はブレードを力学的に解析することにより得られている。この手法の検証は飛行試験空力荷重データから算出されたねじりモーメントやその他のブレードの応答データを用いて行われた。飛行試験データはNASA/Army　UH-60Aブラックホーク空力荷重プログラム(BHAP)から得られた。測定値のランダムエラーに対する同定パラメータの感度を調べるため誤差解析も行われた。結果としてこの方法の有効性が，飛行試験データとの比較を含めた数値計算結果から検証された。
Key words: blade load identification, torsional deformation, inverse transfer matrix method

1. Notation

e　distance between mass and elastic axis, positive when mass lies ahead of elastic axis

e_A distance between area centroid of tensile member and elastic axis, positive when centroid lies ahead

e_o distance at root between elastic axis and axis about which blade is rotating, positive when elastic axis lies ahead

GJ　torsional rigidity

I_η, I_ξ flapwise and chordwise principal mass moments of inertia, respectively

I_θ　torsional mass moment of inertia

k^2_A polar radius of gyration

k_ϕ control system stiffness

ℓ　length of blade segment

M_x, M_a structural and external moment about x axis, respectively

r distance of blade element mass from the center of rotation

T centrifugal tension

X, Y, Z stationary shaft coordinate system or rotating hub coordinate system

x, y, z rotating blade coordinate system

η, ξ direction of the major and minor principal axes, respectively

$\Delta\theta$ built-in twist angle of the blade segment

$\Delta\phi$ change in torsional displacement along blade segment, ℓ

μ rotor advance ratio, $V\cos\alpha/\Omega R$

θ pitch angle of the blade section, positive when leading edge is up

ϕ torsional displacement about x axis, positive when leading edge is up

Ω rotor rotational speed

subscripts and superscripts

n number of blade stations and elements

$(\ddot{\ })$　$d^2(\ )/dt^2$

$(\ )'$　$d(\ )/dr$

2. Introduction

A rotor blade can experience large variations in aerodynamic pitching moment along the blade span during its rotation around the rotor's azimuth. The moments are highly motion dependent and, among other parameters, depend upon the coupled blade

dynamic response and the unsteadiness of the air flow. These moments directly influence the pitch link loads, the overall performance of the rotor, and are strongly governed by blade stall and compressibility effects. For these compelling reasons, to understand and accurately determine these moments has long been a desire and worthy goal of the rotorcraft engineer to bring about a successful rotor design. In response, the rotorcraft industry has focused a great amount of its attention on these physical phenomena experienced by the blade, i.e. dynamic blade stall, as evidenced by the large number of research works available in the literature. In the literature, efforts have been made to understand the nonlinearity of the aerodynamic forces and the wake induced inflow that governs them.

While much work has been done, there is still uncertainty in the results and the methods of prediction. To reexamine the determination of rotor loads, a second method, that of identification is available to determine rotor blade steady and unsteady loads. Though it has not received much attention until recently because of the lack of sufficient flight test data, a few researchers since the 1950's have explored this approach as a way to determine rotor loads. This approach, in recent works, has shown great promise in the accurate determination of rotor blade out-of-plane and in-plane airloads, i.e. References [1, 2, 3]. In the prediction method, noted as the "direct" problem, the airloads are "known" and the blade response is unknown. Conversely, in the identification method or "inverse" problem, the blade response is known and the airloads are unknown.

3. Identification Methodology

Until recently, rotor load identification had focused on the flapwise case only and was based on modal superposition. However, as discussed in Ref. [3] for coupled flap-lag motion, a new approach, which employed the Mykelstad method for the identification of blade loads, had been developed and shown to be much more robust than the modal method. The solution process is based on the "Inverse Transfer Matrix Method" (ITMM) and the equations of motion, based on Reference [4], were developed using the force analysis method. To extend the (ITMM) approach, the Holzer method, Reference [5], is now employed for the identification of the blade spanwise torsional moments. The force analysis method uses torsional moments obtained from experimental data in conjunction with an equilibrium analysis of the aerodynamic and inertial torsion moments to obtain the blade aerodynamic pitching moments (i.e. external moments). The identification methodology then, in this paper, is an approach to determine blade torsion response and external moments from measured structural response data, such as measured strains at specific radial stations on the blade, local rotational accelerations, and/or collective pitch angle measured at the blade root during testing. From the identified torsional loads, the pitch link loads can then be determined. Figure 1. depicts the process for the identification of torsion loads.

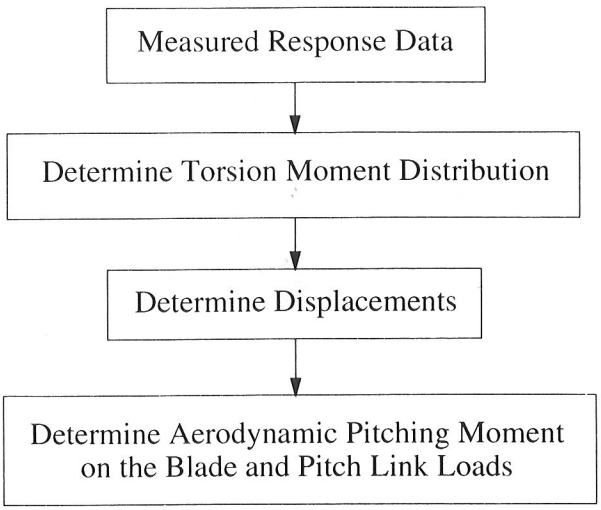

Fig. 1 Rotor Blade Load Identification Using Matrix Transfer Method

4. Torsion Dynamic Model

The hub plane coordinate system is used in the analysis and is represented in Figure 2. The pitch angle θ and elastic torsional displacement ϕ are defined with respect to the hub plane. The model accommodates mass centroid and area centroid axes offsets from the elastic axis which are defined in Figure 3. Also incorporated into the model are the provisions for a torque offset, variable pretwist and nonuniform mass and stiffness section properties. Blade structural damping, sweep and droop, however, are not included.

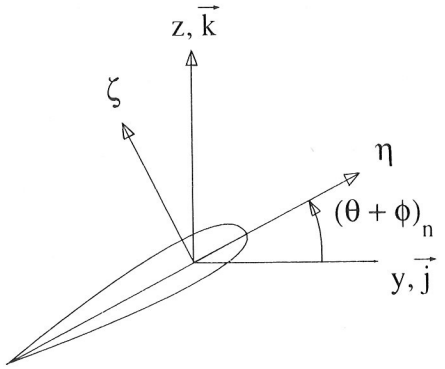

Fig. 2 Hub Frame and Principal Axes Coordinates With Torsional Deformation

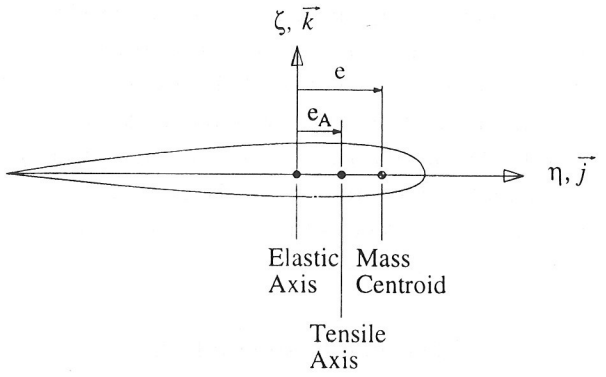

Fig. 3 Blade Structural Parameter Offsets

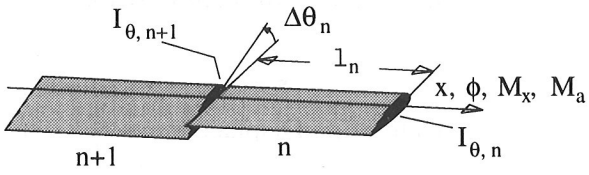

Fig. 4 Adjacent Blade Segments

The set of continuos equations of motion were posed as a set of finite difference equations using a lumped parameter methodology to obtain a solution for the set of differential equations of motion. The lumped parameter technique utilized in this work is a transfer matrix method type of analysis first posed by Holzer in an analysis for the torsional vibration of shafts. The blade is divided into a number of spanwise elements, shown in Figure 4., not necessarily equal in length, each of which consists of a massless elastic beam segment with stiffness GJ and a concentrated inertia.

The blade pitch angle, θ, defined as

$$\theta_n = \theta_o + \theta_{1c}\cos\psi + \theta_{1s}\sin\psi + \theta_{tw,n} \qquad (1)$$

is implemented through the steady and 1st harmonic pitch inputs at the blade root and the blade built-in twist. The process for the variation of the states in the identification methodology is developed such that the analysis advances from the root of the blade to the tip. The states M_x, ϕ, which are located at the right side of the mass station, are represented along the blade at each of the spanwise segments and change in such a manner that the variation can be considered to occur in a series of steps. Within each analysis step from the station n+1 to station n, there are three intermediate steps. The first involves a rotation discontinuity $\Delta(\theta+\phi)_n$ between station n+1 and station n to account for pre-twist and elastic deformation. The second intermediate step, advancing from the left side of the segment to the right, involves movement across the massless elastic nth segment of length ℓ_n and the third involves movement across the nth lumped mass moment of inertia of the nth station.

Based on the process described above, the equations of motion in lumped parameter form, can be developed. To do so, the forces and moments that act on the nth blade segment are determined and the equilibrium of the segment in terms of a set of relations is obtained. These forces and moments are due to aerodynamic, inertia and centrifugal type loadings and arise due to mass offset from the elastic axis and torque offset. The equilibrium of the moments, which include the external moments, and the elastic rotation at the nth blade segment leads to the relations (2) and (3). Equation (5) signify terms due to direct and indirect inertia and centrifugal forces acting on the mass.

$$M_{x,n+1} = M_{x,n} + {}'M_{x,n} + M_{a,n} \qquad (2)$$

$$\phi_{n+1} = \phi_n - \frac{(M_{x,n+1}\,\ell_n + T_{n+1}k_A^2\,\theta'\,\ell_n)}{(GJ_n + T_{n+1}k_A^2)} \qquad (3)$$

where the boundary conditions are

$$M_{x,root} = M_{x,data},\quad \phi = \frac{M_{x,root}}{k_\phi} \text{ and } M_{x,tip} = 0$$

and the centrifugal force along the blade is

$$T_{n+1} = T_n + m_n\Omega^2 r_n. \qquad (4)$$

$$\begin{aligned} {}'M_{x,n} = {} & -m_n\Omega^2 e_n e_o \quad (\sin\theta_n + \phi_n\cos\theta_n) \\ & - I_{\theta,n}\ (\ddot{\phi}_n + \ddot{\theta}_n) \\ & - \Omega^2(I_{\xi,n} - I_{\eta,n})\ \ (\phi_n\cos 2\theta_n + \sin\theta_n\cos\theta_n) \end{aligned} \qquad (5)$$

The external pitching moment can then be obtained

$$\begin{aligned} M_{a,n} = {} & M_{x,n+1} - M_{x,n} + I_{\theta,n}\ (\ddot{\phi}_n + \ddot{\theta}_n) \\ & + m_n\Omega^2 e_n e_o(\sin\theta_n + \phi_n\cos\theta_n) \\ & + \Omega^2\ (I_{\xi,n} - I_{\eta,n})\ \ (\phi_n\cos 2\theta_n + \sin\theta_n\cos\theta_n) \end{aligned} \qquad (6)$$

5. Method Of Solution

In this analysis only the steady state solutions are sought. It is therefore assumed that the steady state response of a rotor blade is periodic so a harmonic solution is applied to the equations of motion. These harmonics are of the form $a_{\varkappa c}\cos(\varkappa\Omega t) + a_{\varkappa s}\sin(\varkappa\Omega t)$ and result in a separate set of identified parameters for each $\varkappa$ harmonic where $\omega = \varkappa\Omega$. The torsional deformation, ϕ_n can readily be identified through the use of the experimental torsion strain measures. Using the torsional moment, $M_{x,n}$, the torsional deformations are identified as the solution transfers from the blade torsion bearing to the tip. The process is initiated using the boundary condition at the root, $\phi_{root} = M_{x,root}/k_\phi$. With the elastic torsion deformation known, the spanwise external pitching moments can be identified for a given harmonic.

6. Results And Conclusion

The UH-60A main rotor was used as the model in the method verification and the identification analysis. The UH-60A main rotor geometric and structural properties were obtained from NASA Ames Research Center and the external moment data, used for verification, were obtained from flight test as part of the NASA/Army UH-60A Black Hawk Airloads Program (BHAP). The UH-60A main rotor blade has an aft swept tip which was ignored in the analysis.

The torsion bearing was assumed to be co-located with the flap and lag elastomeric bearing and the main rotor blade was discretized into 48 spanwise elements for a total of 49 radial stations. The outer 48 radial stations along the blade, r=.06R to 1.0R, are equally spaced while the 49th station was placed at .0466R to coincide with the focal point of the elastomeric bearing. The lengths of the outer 47 elements is ℓ =.02R and the inner most element between station 48 and 49 has a length of ℓ =.0134R. The built-in blade twist, which washes out in a linear manner for most of the blade, has a positive slope beyond .94 R. The control system stiffness, k_ϕ, was assumed to be linear.

In the analysis, it is desirable to use torsion moments obtained from experimental data to determine the spanwise external moments. However, due to limitations in the BHAP torsion strain measure data, these data were not utilized. Consequently, to obtain the distributed torsional moments, simulation was used and to generate these data sets, a prediction methodology was employed. The simulated distributed torsional moments were generated using the torsion equations from Reference [4] in the form of the Transfer Matrix Method (TMM) and the BHAP airloads data were used as the forcing function. To validate this structural dynamics model, the modes and frequencies from the prediction analysis were checked for agreement with the results from CAMRAD/JA noted in Reference [6]. CAMRAD/JA computes only nonrotating torsion modes so their solution is independent of rotor speed or collective pitch. Also in CAMRAD/JA, only the cantilever beam case is considered for torsion. Table 1 and Figure 5. provide the eigenvalues and eigenvectors. The identification analysis only considered the first 10 harmonics (including the steady term) and the TMM correlates very well for this frequency range.

The identification process of the rotor blade's external moments depends on, among other things, the accurate identification of the blade's displacements. To obtain confidence in the identified moments and the methodology itself, a second validation exercise

Table I Comparison of Eigenvalues: Transfer Matrix Method (TMM) vs. CAMRAD/JA, Torsion Modes (Per Rev), Rigid Root

	TMM	CAMRAD/JA
Mode	**Torsion**	**Torsion**
1	5.333	5.357
2	4.895	4.905
3	15.657	15.109
4	25.992	25.098
5	36.444	36.765
6	47.755	50.813
7	67.681	69.645
8	##	##
9	##	##
10	##	##

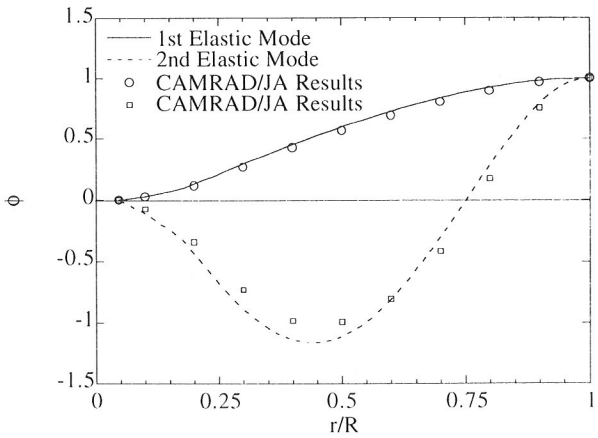

Fig. 5 Modal Analysis: Transfer Matrix Method vs. CAMRAD/JA, 1st and 2nd Elastic Torsion Modes, Rigid Root

was conducted at a midpoint in the solution process. As such, the identified blade torsional displacements, fn, were correlated with the simulated data from the response methodology. The identification methodology for the UH-60A employed the simulation data for the flight conditions, μ=0. and μ=0.193. The air density and rotor speed, corresponding to the two flight conditions, were used. For each respective flight condition, the identification analysis was performed at two rotor azimuthal positions, ψ=0. and ψ=90. deg. Figures 6 and 7 provide examples for the steady and first harmonic cosine displacement coefficients at two different advance ratios. One set of parameter curves, in each figure, are the simulated data and are considered to be an "exact" set of measurements which are labeled as "Data" and are referred to as"measured data". The other set of parameter curves are the data generated from the identification methodology and are labeled as "Identification". As can be seen, the correlation between the measured data and the identified results are excellent.

The results from the analysis of the distributed

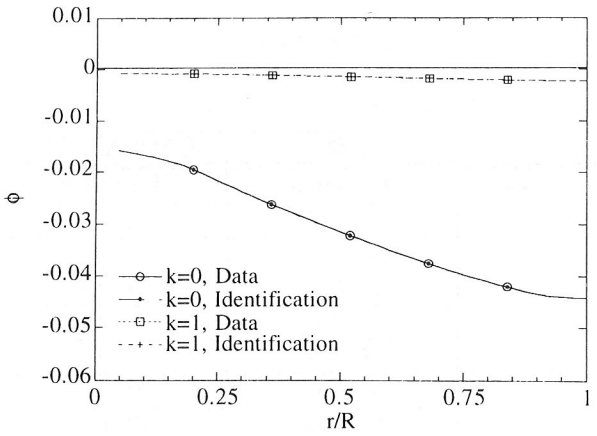

Fig. 6 Nondimensionalized Torsional Displacement, Zeroth and First Harmonic, $\mu=0.$, $\psi=0.$ deg.

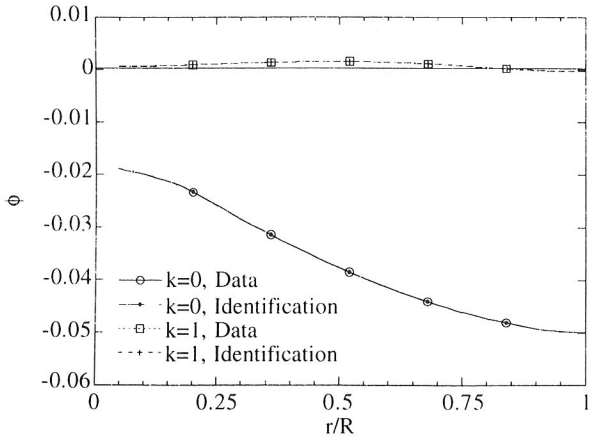

Fig. 7 Nondimensionalized Torsional Displacement, Zeroth and First Harmonic, $\mu=0.193$, $\psi=0.$ deg.

external moments, $M_{a,n}$ are next correlated with experimental flight test data from the UH-60A flight test program as shown in Figures 8 through 11. A range of harmonics and examples of ψ=0, 90 deg. are shown. In each figure, one set of parameter curves are the UH-60A airloads flight test data which are an exact set of measurements and are labeled as "Flight Test". The other set of parameter curves are the corresponding external moments generated from the identification methodology and are labeled as "Identification". The external moment, $M_{a,n}$ which is in per unit length in the analysis, has been nondimensionalized for presentation by the factor $\rho(\Omega R)^2 \bar{c}^2$. Again, it can be seen that the correlation between the flight test data and the identified results are excellent.

The results provided above, in general, have an excellent correlation with the experimental data provided therein. However, since random errors, in the form of noise, in the simulated data does not exist, the results are not fortuitous and are an inevitable out-

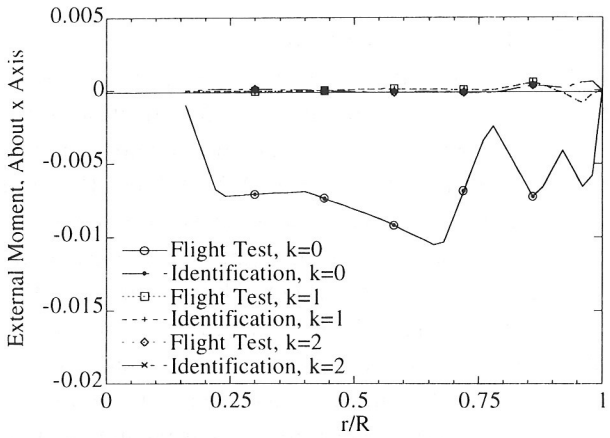

Fig. 8 Nondimensionalized Identified External Moment About x Axis, Zeroth, First and Second Harmonic, $\mu=0.$, $\psi=0.$ deg.

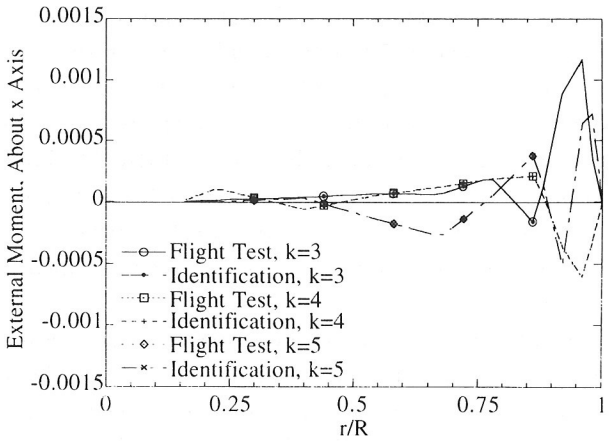

Fig. 9 Nondimensionalized Identified External Moment About x Axis, Third, Fourth and Fifth Harmonic, $\mu=0.$, $\psi=0.$ deg.

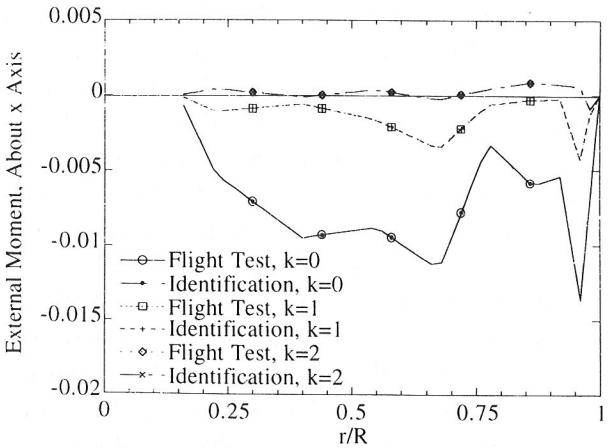

Fig. 10 Nondimensionalized Identified External Moment About x Axis, Zeroth, First and Second Harmonic, $\mu=.193$, $\psi=90.$ deg.

come. Since, noise can influence the experimental data, an error analysis was performed to investigate the sensitivity of the identified parameters to random errors of measured data. The error analysis was performed in a realistic sense with the simulated torsion moments perturbed at only 8 radial locations.

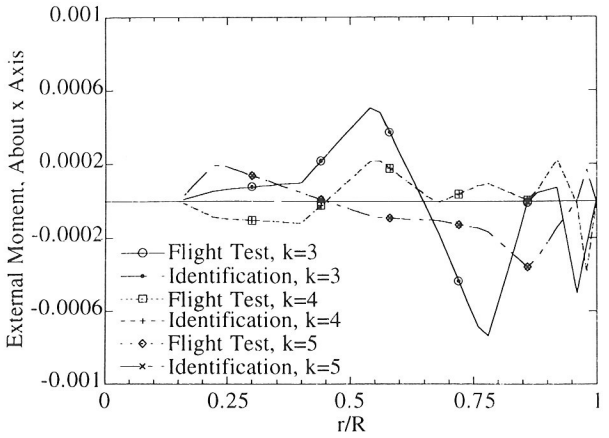

Fig. 11 Nondimensionalized Identified External Moment About x Axis, Third, Fourth and Fifth Harmonic, $\mu=.193$, $\psi=90.$ deg.

The sensor location points were equally spaced at .1 R intervals from r=.2R to r=.9R where it is noted that these points coincided with specific calculation points on the blade. Two error cases were investigated and consisted of a ±2 percent random error and a ±5% random error, respectively. The errors consisted of a set of 8 amplification factors biased about zero and having a total amplitude of 4% and 10%, respectively. The external loads were identified for these two error cases. The blade displacements are very insensitive, however, to perturbations and as such, only the 5% random error case was considered as shown in Figure 12. Figure 13 presents the ±2% random error case for the results of the external moments. The results show that the random noise can have a fairly large influence on the steady harmonic of the identified external moments. Reference [3] addresses a technique, based on an error analysis strategy, which can be used to limit the errors and provide a reasonable moment distribution. This technique was not applied in this analysis due to space constraints.

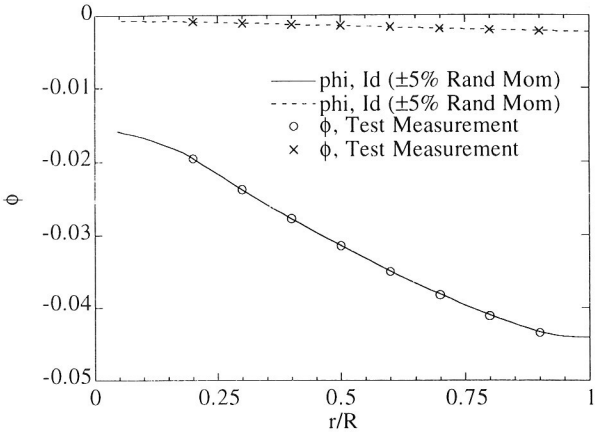

Fig. 12 ±5% Random Error on Moments at 8 Points, Nondimensionalized Torsion Displacement, Zeroth and First Harmonic, $\mu=0.$, $\psi=0.$ deg.

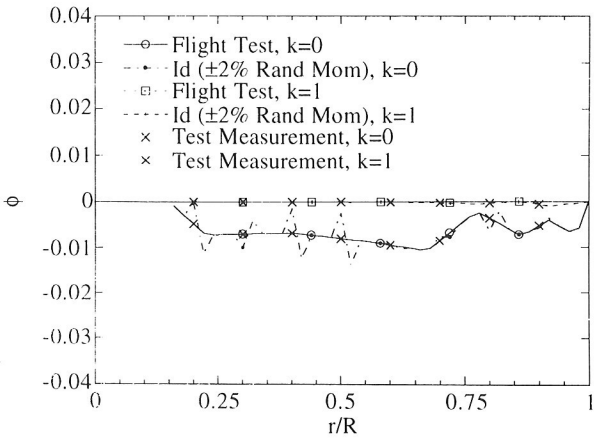

Fig. 13 ±2% Random Error on Moments at 8 Points, Nondimensionalized Identified External Moment About x axis, Zeroth and First Harmonic, $\mu=0.$, $\psi=0.$ deg.

7. References

[1] Liu, S., Higman, J.P. and Schrage, D.P.,"On The Determination Of Helicopter Rotor Loads," Proceedings of the Aeromechanics Specialist Conference, AHS, San Francisco, CA, January, 1994.

[2] Liu, S., Higman, J.P. and Schrage, D.P., "On the Displacement and Load Determination of a Helicopter Rotor Blade With And Without Higher Harmonic Control," Twentieth ERF, Amsterdam, The Netherlands, October 4-7 1994.

[3] Liu, S., Higman, J.P and Schrage, D.P.,"Coupled Flap-Lag Rotor Blade Load Identification," Proceedings of the 51st Annual AHS Forum, May 1995.

[4] Houbolt, J.C. and Brooks, G.W.,"Differential Equations of Motion for Combined Flapwise Bending, Chordwise Bending and Torsion of Twisted Nonuniform Rotor Blades, "NACA Rep. 1346, 1958.

[5] Holzer, H., "The Calculation of Rotational Harmonic Motion (In German)," Berlin, Springer Verlag, 1921.

[6] Johnson, W., "A Comprehensive Analytical Model of Rotorcraft Aerodynamics and Dynamics", Johnson Aeronautics Version, Vol. I : Theory Manual, Palo Alto, CA, 1988.